3D printed thermo-responsive electroconductive hydrogel and its application for motion sensor

Yangyang Li, Wenhui Zheng, Jichi Zhang, Lijuan Xu, Bing Li, Jidong Dong, Guo-Lin Gao* and Zaixing Jiang*

MIIT Key Laboratory of Critical Materials Technology for New Energy Conversion and Storage, School of Chemistry and Chemical Engineering, Harbin Institute of Technology, Harbin, China

Stimulus-responsive hydrogels with excellent conductivity have been widely used in electrical, electrochemical, biomedical, and other fields. It is still a challenge to prepare gels with high conductivity. In this paper, poly (N-isopropyl acrylamide) is 3D printed by changing the rheological properties of the printing solution with clay. By forming phytic acid cross-linked polyaniline conductive polymer network *in situ* on the poly (N-isopropyl acrylamide) matrix, 3D printing of thermally responsive conductive hybrid hydrogels was realized. The interpenetrating polymer network structure provides an electron transport path for hydrogels. The hydrogels have high porosity, strong interaction, high electrical conductivity, high thermal response sensitivity, and significant mechanical enhancement. The results show that the swelling and mechanical properties of the gel are influenced by soaking in different concentrations. The application scenario of the hydrogel was confirmed by a temperature-sensitive switch and finger motion detection.

Introduction

Stimulus-response gels are functional hydrogels that respond to external signals, such as temperature, (Li et al., 2011), PH, (Li et al., 2014), electric field, (Yang et al., 2011; Annabi et al., 2014), magnetic force, (Zhai et al., 2013), and so on. 3D printing of functional gels can be used in a wide range of applications. Traditional response gels tend to respond to only one source. The multi-response and multi-function intelligent gel materials have a wider range of application scenarios, such as intelligent sensors, intelligent robots, flexible wearables, and other fields. Thermosensitive conductive gel is a kind of conductive gel that is sensitive to temperature. He can feel the stimulation of temperature changes in the outside world and translate it into electrical signals. This can be widely used in smart clothing, real-time monitoring, and other fields.

In recent years, flexible sensors have been widely paid attention to and used in electronic skin (Gao et al., 2019), soft robots (Treml et al., 2018), artificial intelligence (Fernandes et al., 2019), health monitoring (Wu et al., 2020), and other fields. Flexible sensors need excellent mechanical properties, high sensitivity, good stability and repeatability. Conductive hydrogels have good flexibility and biocompatibility, which make them a rational flexible sensor material. Traditional hydrogels are generally non-conductive. The prepared conductive hydrogels usually introduce a second component into the collective of traditional hydrogels to conduct electricity. Such as conductive filler, conductive polymer, etc., Pan et al. (2012) introduced a conductive polymer network into the

traditional NIPAM gel collective to prepare polyaniline and polypyrrole, which realized the conductive characteristics of the temperature-sensitive gel. Qin et al. (2022) introduced LiCl into polyacrylamide/hydroxypropyl methylcellulose (PAM/HPMC) composite hydrogel, A method for the rapid synthesis of N, N-dimethyl acrylamide-Paam/Ca hydrogels (MBAA-PAAM/Ca gels) sensors using a "one-pot method" has been reported by Bai et al. (2021) PAAM hydrogel has the characteristics of low raw material cost, uniform polymerization, good transparency, and non-toxic. Bai et al. (2020) report on a new transparent and highly ionic conductivity hydrogel that regulates the crosslinking interaction of hydrogel networks by introducing biomineral calcium ions into the pam Sodium carboxymethylcellulose (CMC) crosslinking network. The hydrogel integrates high strength, high tensile, and self-adhesive skin sensor-like properties.

3D printed hydrogels have been extensively studied in recent years Boere et al. (2015) present a new bio ink for 3D printing, capable of forming large, highly defined constructs. Abbadessa et al. (2016) design a hydrogel system based on methacrylate chondroitin sulfate (CSMA) and a thermo-sensitive poly [N-(2-hydroxypropyl) methacrylamide-mono/dilactate]-polyethylene glycol triblock copolymer (M15P10) as a suitable material for additive manufacturing of scaffolds. Because polymers are by far the most utilized class of materials for 3D printing additive manufacturing, Ligon et al. (2017) focus on polymer processing and the development of polymers and advanced polymer systems specifically for AM. Polymer designs that meet the rheological requirements for direct ink writing are outlined and successful examples are summarized, which include the development of polymer micelles, co-assembled hydrogels, supramolecular cross-linked systems, polymer liquids with microcrystalline domains, and hydrogels with dynamic covalent cross-links Li et al. (2019) SiO nanoparticles are loaded into alginate-gelatin composite hydrogels and chemically crosslinked with CaCl solution Roopavath et al. (2019). Cristovao et al. (2019) combine chemical and UV laser polymeric cross-linkage to control the mechanical properties of 3D-printed hydrogel blends. Without imitating dynamic movements, there are limitations on the extent to which the proper implementation of the tissue's own functions can be achieved.

In this paper, the conductive polymer hydrogel was introduced into the preprinted thermosensitive hydrogel poly (N-isopropyl acrylamide) (PNIPAM), and the conductive smart gel sensitive to temperature change was developed. Phytic acid molecules can protonate nitrogen groups on the PANI molecular chain, and a single phytic acid molecule can react with multiple PANI molecular chains. In this way, a conductive gel network can be in-situ polymerized inside the printed PNIPAM gel. The effect of two gel networks can greatly improve the mechanical properties of the gel. The inner porous and loose morphology provides a way for water molecules to flow. The hybrid gels we obtained have excellent temperature sensitivity and electrical conductivity.

Results and discussion

Smart gels have broad applications. Traditional smart hydrogels are generally electrically non-conductive. Few relevant types of research focus on the preparation of conductive gels through 3D printing. In this paper, a 3D printable thermo-sensitive conductive gel was prepared by in-situ polymerization, and the target shape of the thermo-sensitive gel matrix was prepared by 3D printing. The thermo-sensitive gel matrix was immersed in a mixture of water and ethanol containing aniline monomer. The initiator and phytic acid promote the polymerization of aniline monomer.

The aniline monomer was in-situ polymerized within the molecular chain of Poly (N-Isopropyl acrylamide) (PNIPAM) by the action of initiator and phytic acid to form a conductive polyaniline network. Phytic acid is a kind of natural substance that exists widely in plants and has abundant yield. Phytic acid reacts with the Pani chain by protonating the nitrogen group. A single phytic acid molecule can react with multiple polyaniline molecular chains simultaneously to form a conductive network. As shown in Figure 1, the aqueous solution of NIPam is thin and not suitable for direct extrusion printing. The rheological modifier lapnito XLG, a 10 nm nm sheet, is distributed directly in water to increase the viscosity of the water. The clay-thickened NIPAM solution can be extruded directly. Nipam gel after 3D printing has certain temperature sensitivity. When the phase transition temperature was higher than 35°C, the molecular chain of NIPAM was curled and the gel volume shrank. The shrunk gel is then immersed in a mixture of water and ethanol containing aniline monomers. Under the condition of the lower phase transition temperature, the molecular chain of NIPAM stretched and the gel volume swelled. In the process of swelling, the gel sucked the surrounding mixed solution into the gel network, during which the aniline monomer was dispersed within the molecular network of Nipam. Phytic acid molecules are linked by inducing the protonation of nitrogen groups on aniline. In this process, a single phytic acid molecule reacts with multiple nitrogen groups to form a polyaniline network. The polyaniline network provides a transmission path for electron transport and forms an in-situ polymerized gel conducting network on the NIPAM molecular chain.

Figure 1A shows the real pictures of the gel in each process. The initial PNIPAM was a transparent gel after being printed and cured. The aniline monomer is absorbed inside the gel after being soaked in an aniline water/ethanol solution. The gel is light yellow. In the last step, the sample was transferred to phytic acid solution, and the aniline monomer was in-situ polymerized within the PNIPAM gel network to form a polyaniline network. The whole sample was brown, and a few parts were green. The chemical structure of the PNIPAM/PANI hybrid gel was analyzed by Fourier transform infrared spectroscopy (FTIR). Figure 1B shows the FTIR spectra of PANIPAM, the gel after swelling of aniline absorption monomer, and the hybrid gel after in-situ polymerization of aniline monomer (PNIPAM/PANI). In the spectrum of PNIPAM, the two characteristic absorption peaks of PNIPAM are 1,540 cm^{-1} and 1,654 cm^{-1}, respectively. They are attributed to the bending vibration of the N-H bond and the stretching vibration of C=O, respectively. After the swelling and absorption of the aniline monomer, the absorption vibration peak of the benzene ring appeared at 1,480 cm^{-1}. After in-situ polymerization, a quinone ring at 1,570 cm^{-1} was formed. All characteristic absorption peaks of PNIPAM and PANI could be found in the whole synthesis process. That proved the formation of the PNIPAM/PANI hybrid gel.
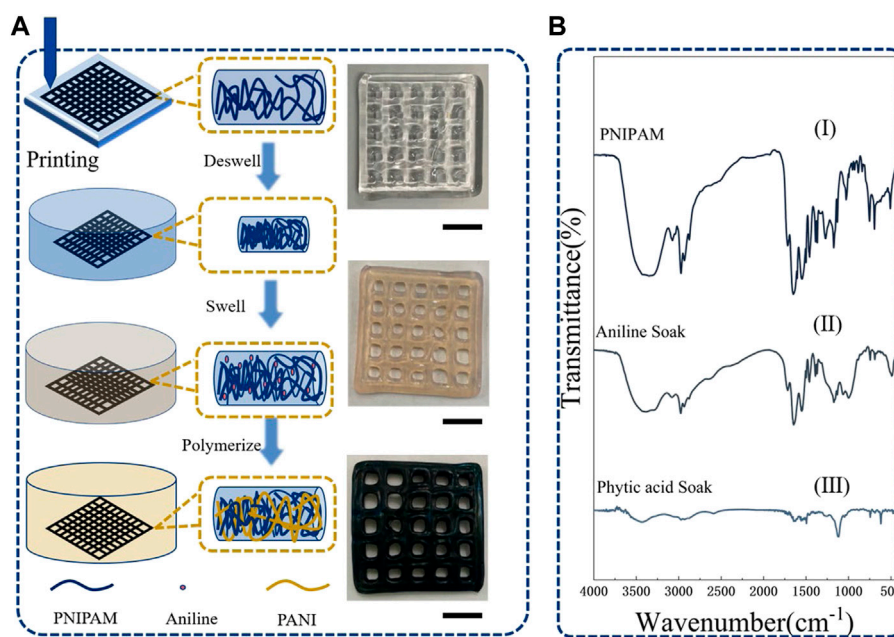
FIGURE 1
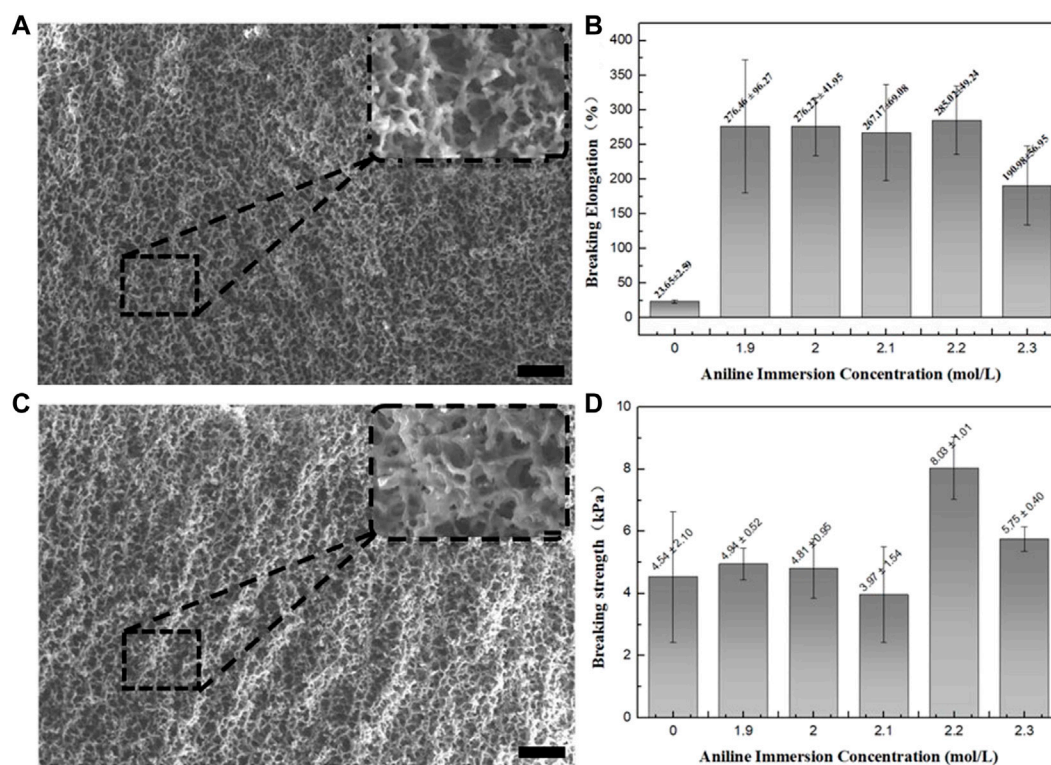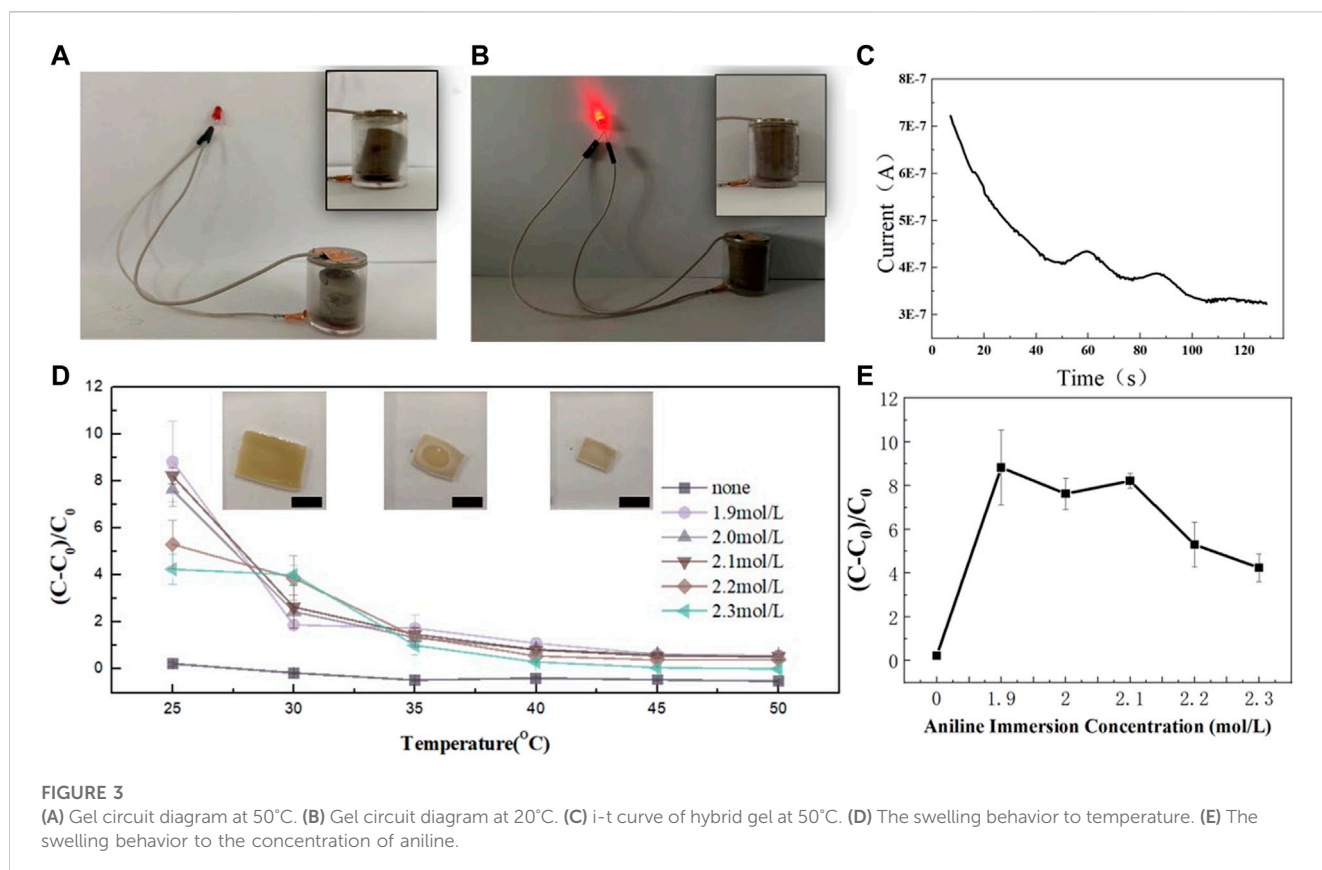**(A)** The preparation process of hybrid gel, **(B)** FTIR spectra of different stages of gel, the ruler is 1 cm.

FIGURE 2
(A) SEM image of 1.9 mol/L sample, **(B)** Elongation at break. **(C)** SEM image of 2.3 mol/L sample. **(D)** Tensile fracture strength.

FIGURE 3
(A) Gel circuit diagram at 50°C. **(B)** Gel circuit diagram at 20°C. **(C)** i-t curve of hybrid gel at 50°C. **(D)** The swelling behavior to temperature. **(E)** The swelling behavior to the concentration of aniline.

In this paper, the author prepared hybrid gels under different conditions by changing the concentration of aniline. The possibility of regulating the mechanical properties of hybrid gels by changing aniline concentration was explored. The concentration of aniline monomer was 1.9 mol/L, 2.0 mol/L, 2.1 mol/L, 2.2 mol/L, and 2.3 mol/L, respectively. The microstructure and morphology of the hybrid gel were studied by scanning electron microscopy (SEM). Figures 2A, C show the SEM image of the hybrid gel samples at 1.9 mol/L and 2.3 mol/L. The gel samples were freeze-dried, and the fracture surface was tested. As can be seen in the figure, the hybrid gel presents a porous structure inside. Pore size is evenly distributed, ranging from a few microns to more than 10 microns in size. The pores show a hierarchical porous structure. This special morphology provides a nanoscale transmission channel. Water molecules are transported freely through the channels. The aniline molecules could follow the mixed solution into the gel network, during the swelling process. After aggregation, a PANI network was formed on the PNIPAM network. It can be seen by comparing Figures 2A, C the overall structure of the gel network is similar, with little difference in pore diameter. Similarly, the same result can be obtained by comparing other samples (Supplementary Figure S2). The results showed that the microstructure of the polymer network skeleton was not affected by the change of aniline concentration.

Mechanical properties are an important indicator of hydrogels as sensors. Hydrogels have general mechanical strength because of their porous and loose structure. Figure 2B shows the comparison of elongation at the break of different samples. The graph shows that there has been a steep increase in elongation at the break of the hybrid gel. The elongation at break of PANIM was only 23.65% ± 2.59%, and the tensile fracture strength was 4.54 ± 2.10 kpa. The hybrid gel formed by different concentrations of aniline immersion has a significant increase in elongation at break. The elongation at break of sample 1.9 mol/L, 2.0 mol/L, 2.1 mol/L, 2.2 mol/L and 2.3 mol/L reached 276.46% ± 96.27%, 276.22% ± 41.95%, 267.17% ± 69.08%, 285.02% ± 49.24%, 190.98% ± 56.95%, respectively. Compared with the PNIPAM, the elongation at break was increased by 10 times after hybridization. One reason why elongation have increased is that the introduction of the PANI network formed two networks inside the gel. The PANI polymer network dispersed the external forces to some extent during the stretching process. It is also worth noting that the concentration of aniline does not have a great effect on the elongation at break of the hybrid gel. Figure 2D is the comparison of tensile fracture strength of different samples. The fracture strength of samples 1.9 mol/L, 2.0 mol/L, 2.1 mol/L, 2.2 mol/L and 2.3 mol/L was 4.94 ± 0.52 kPa, 4.81 ± 0.95 kPa, 3.97 ± 1.54 kPa, 8.03 ± 1.01 kPa, 5.75 ± 0.40 kPa, respectively. Compared with the PNIPAM gel, the fracture strength of the hybrid gel was almost the same. When the gel was stretched to an extreme position, the PNIPAM polymer chain still played a major role. The introduction of PANI network did not enhance the fracture strength of the gel. Compared with PNIPAM gel, hybrid gel significantly enhanced the elasticity of the gel due to PANI. In the meantime, the change of aniline concentration has little effect on the mechanical properties of the final hybrid gel.
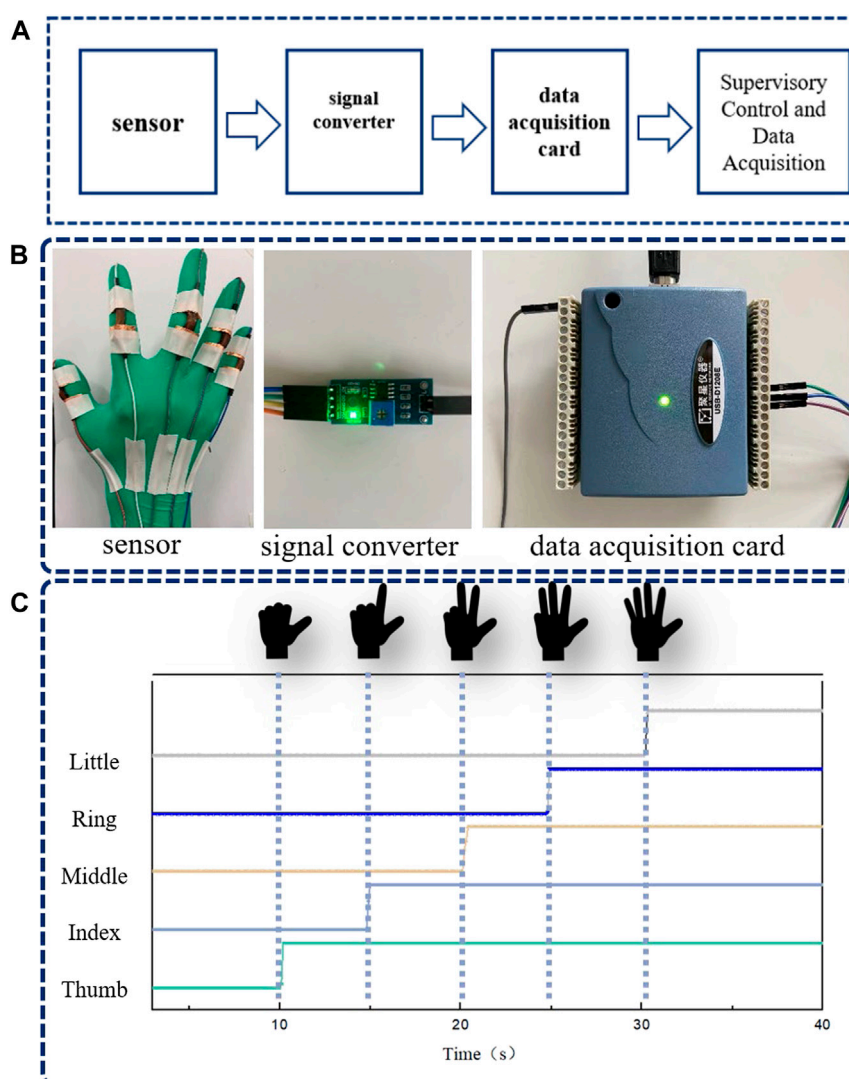
FIGURE 4
(A) Signal transmission flow of sensing device. **(B)** The physical image of the sensor device. **(C)** Signal display of different gestures.

Water absorption swelling is an important characteristic of hydrogels. PNIPAM gel is very sensitive to temperature change. As shown in Figure 3D, PANIPAM gel demonstrates rapid water-loss shrinkage and size smaller with the temperature increases. Figure 3D (I–III) recorded the process of the gel's shrinkage in 50°C water. Figure 3D shows the curve of gel swelling from 25°C to 50°C water. Compared with PANIPAM, the temperature sensitivity of PANIPAM/PANI is significantly enhanced. In addition, the volume shrinkage of all hybrid gels is basically completed near lower critical solution temperature (LCST) (35°C). In a water temperature higher than 40°C, the volume change tends to be stable. Figure 3E shows the swelling capacity of the different samples at room temperature. The PNIPAM/PANI has a higher swelling capacity than the PNIPAM. What can be clearly seen in this figure is the steady decline of swelling capacity with the increase of soaking concentration. However, the downward trend is not very obvious.

Due to the *in-situ* polymerization of pani molecular chain within the gel network of Anupam, the conductive pani molecular chain

shifted following the shrinking process of pnipam molecular chain after the temperature increased, and the electrical conductivity also changed. Figure 3C shows the hybrid gel pasted on the outer wall of the beaker. An electrochemical workstation was used to test the i-t curve of the hybrid gel after 50°C hot water was added to the beaker. After hot water is added to the beaker, the hybrid gel attached to the beaker wall feels the temperature rise, and the volume of the hybrid gel changes, the pani molecular chain that carries electricity changes, causing the resistance value to increase and the current to decrease. This experiment confirms the thermosensitive conductivity of hybrid gels and provides the application scenario of hybrid gels as thermosensitive sensors.

The hybrid gels themselves have temperature-sensitive and conductive properties. Figures 3A, B show the application scenario of hybrid gel as a temperature-sensitive sensor. As shown in Figure 3A, a hybrid gel of a specific size and shape is placed in a sealed cylindrical container. At normal temperature, the upper part of the hybrid gel is in contact with the negative electrode

of the button battery. The lower part is connected with the light-emitting diode through copper tape. The whole form conductive circuit. When the gel is heated, the gel dehydrating volume shrinks. The top of the gel loses contact with the button battery. The whole circuit is disconnected (Figure 3B). The hybrid gel acts as a switch throughout the circuit. When the temperature is lower than LCST, the gel is in a swelling state. The circuit closes and the diode lights up. When the temperature is higher than LCST, the gel de-solubilization and volume becomes smaller. The circuit is on, the diode is off. Due to the excellent thermal response sensitivity of the hybrid gel, the whole state switch is very fast. Figure 3C shows the loop current change curve of PNIPAM/PANI during the process of shrinking. PNIPAM/PANI gel is attached to the outer wall of the beaker. An electrochemical workstation was used to monitor the current curve in the gel in. At 0 s, 50°C water was added into the beaker. Then, the gel loses water. Over time, the current in the gel decreases. This experiment confirmed the thermosensitive conductivity of the gel. The application prospect of thermosensitive gel as a thermosensitive sensor is provided.

The proposed sensor has been confirmed to have the potential to monitor human motions. For a practical application, a smart glove for real-time motion detection was assembled, as shown in Figure 4. The smart glove was composed of five strain sensors, a signal converter, and a data acquisition card. The data acquisition card was connected to Supervisory Control and Data Acquisition (SCDA). The sensors were mounted onto the finger joints of a rubber glove by tape to detect the signal of each finger, as shown in Figure 4. The entire circuit can be roughly divided into four parts: Sensor, signal converter, data acquisition card, supervisory control, and data acquisition (SCDA), as shown in Figures 4A, B. Ten current leads were led out from five sensors and all connected to the SCDA eventually through a data acquisition card. After the computer received the data, it drew data graphs in real-time through SCDA. The response of each finger was distinct and independent, as shown in Figure 4C.

Conclusion

In conclusion, we successfully prepared PNIPAM gel through 3D printing. In addition, the conductive polymer network PANI was in-situ polymerized on the PNIPAM matrix by phytic acid. The inter-permeable binary polymer network made the hybrid hydrogel show unique characteristics. Hybrid gels have excellent tensile properties, sensitive temperature sensitivity, and electrical conductivity. The application scenario of our gel as a temperature-sensitive sensor was demonstrated by a simple two-stage tube circuit. The effect of aniline concentration on swelling and mechanical properties of hybrid gel was investigated. We have designed a device for real-time hand monitoring. This device can monitor palm movement in real time according to the signals transmitted by the sensor made of gel. This work may have a wide range of applications in stimulus-response electronics, flexible electronics, artificial intelligence wearables, etc.

Experimental section

The ink formula contained n-isopropyl acrylamide (NIPAM), diphenyl (2,4, 6-trimethyl benzoyl) phosphine oxide (TPO) as UV initiator, and Laponite XLG nanosheet as a rheological modification. Dissolve the platinum XLG in 10 mL deionized water and stir with other reagents. All chemicals were purchased from Sigma-Aldrich. Food bot food 3D printer extrusion printing molding. A 365 nm UV light source was used for photocuring molding The printed NIPAM gel was soaked in deionized water for 48 h to remove the unreacted impurities. NIPAM gel was soaked in 60°C hot water to shrink, and then the shrunk gel sample was soaked in an aniline water/ethanol mixture for 24 h to fully expand, the volume ratio of water to ethanol was 1:1. NIPAM gel, fully swollen by aniline solution, was transferred to 13 wt% phytic acid solution to form a polyaniline network in situ.

Data availability statement

The original contributions presented in the study are included in the article/Supplementary Material, further inquiries can be directed to the corresponding authors.

Author contributions

YL: Conceptualization, methodology, writing—original draft preparation WZ: Methodology, software, JZ: Methodology, software, LX: Methodology, software, BL: Validation, formal analysis, JD: Methodology, G-LG: Writing—review and editing, supervision ZJ: Writing—review and editing, supervision.

Funding

Conflict of interest

The authors declare that the research was conducted in the absence of any commercial or financial relationships that could be construed as a potential conflict of interest.

The handling editor (YU) declared a shared affiliation with authors (YL, JZ, LX, BL, JD, G-LG, and ZJ) at the time of the review.

Publisher's note

All claims expressed in this article are solely those of the authors and do not necessarily represent those of

Supplementary material

The Supplementary Material for this article can be found online at: https://www.frontiersin.org/articles/10.3389/fmats.2023.1096475/full#supplementary-material

References

Abbadessa, A., Blokzijl, M. M., Mouser, V. H., Marica, P., Malda, J., Hennink, W. E., et al. (2016). A thermo-responsive and photo-polymerizable chondroitin sulfate-based hydrogel for 3D printing applications. *Carbohydr. Polym.* 149, 163–174. doi:10.1016/j.carbpol.2016.04.080

Annabi, N., Tamayol, A., Uquillas, J. A., Akbari, M., Bertassoni, L. E., Cha, C., et al. *Adv. Mater.* 2014, 25th anniversary article: Rational design and applications of hydrogels in regenerative medicine, 26, 85–124. doi:10.1002/adma.201303233

Bai, J., Wang, R., Ju, M., Zhou, J., Zhang, L., and Jiao, T. (2020). Facile preparation and high performance of wearable strain sensors based on ionically cross-linked composite hydrogels. *Sci. China Mater.* 64, 942–952. doi:10.1007/s40843-020-1507-0

Bai, J., Wang, R., Wang, X., Liu, S., Wang, X., Ma, J., et al. (2021). Biomineral calcium-ion-mediated conductive hydrogels with high stretchability and self-adhesiveness for sensitive iontronic sensors. *Cell. Rep. Phys. Sci.* 2, 100623. doi:10.1016/j.xcrp.2021.100623

Boere, K. W. M., Blokzijl, M. M., Visser, J., Linssen, J. E. A., Malda, J., Hennink, W. E., et al. (2015). Biofabrication of reinforced 3D-scaffolds using two-component hydrogels. *J. Mater Chem. B* 3, 9067–9078. doi:10.1039/c5tb01645b

Cristovao, A. F., Sousa, D., Silvestre, F., Ropio, I., Gaspar, A., Henriques, C., et al. (2019). Customized tracheal design using 3D printing of a polymer hydrogel: Influence of UV laser cross-linking on mechanical properties. *3d Print. Med.* 5, 12. doi:10.1186/s41205-019-0049-8

Fernandes, D. F., Majidi, C., and Tavakoli, M. (2019). Digitally printed stretchable electronics: A review. *J. Mater. Chem. C* 7, 14035–14068. doi:10.1039/c9tc04246f

Gao, W., Ota, H., Kiriya, D., Takei, K., and Javey, A. (2019). Flexible electronics toward wearable sensing. *Accounts Chem. Res.* 52, 523–533. doi:10.1021/acs.accounts.8b00500

Li, D., Zhang, X. Y., Yao, J. F., Simon, G. P., and Wang, H. T. (2011). Stimuli-responsive polymer hydrogels as a new class of draw agent for forward osmosis desalination. *Chem. Commun.* 47, 1710. doi:10.1039/c0cc04701e

Li, L., Lin, Q., Tang, M., Duncan, A. J. E., and Ke, C. (2019). Advanced polymer designs for direct-ink-write 3D printing. *Chemistry-A Eur. J.* 25, 10768–10781. doi:10.1002/chem.201900975

Li, P. J., Yuan, S. S., Tang, Q. W., and He, B. L. (2014). Robust conducting gel electrolytes for efficient quasi-solid-state dye-sensitized solar cells. *Electrochimica Acta* 137, 57–64. doi:10.1016/j.electacta.2014.04.093

Ligon, S. C., Liska, R., Stampfl, J., Gurr, M., and Muelhaupt, R. (2017). Polymers for 3D printing and customized additive manufacturing. *Chem. Rev.* 117, 10212–10290. doi:10.1021/acs.chemrev.7b00074

Pan, L., Yu, G., Zhai, D., Lee, H. R., Zhao, W., Liu, N., et al. (2012). Hierarchical nanostructured conducting polymer hydrogel with high electrochemical activity. *Proc. Natl. Acad. Sci. U. S. A.* 109, 9287–9292. doi:10.1073/pnas.1202636109

Qin, Z., Liu, S., Bai, J., Yin, J., Li, N., and Jiao, T. (2022). Ionic conductive hydroxypropyl methyl cellulose reinforced hydrogels with extreme stretchability, self-adhesion and anti-freezing ability for highly sensitive skin-like sensors. *Int. J. Biol. Macromol.* 220, 90–96. doi:10.1016/j.ijbiomac.2022.08.055

Roopavath, U. K., Soni, R., Mahanta, U., Deshpande, A. S., and Rath, S. N. (2019). 3D printable SiO$_2$ nanoparticle ink for patient specific bone regeneration. *RSC Adv.* 9, 23832–23842. doi:10.1039/c9ra03641e

Treml, B. E., McKenzie, R. N., Buskohl, P., Wang, D., Kuhn, M., Tan, L.-S., et al. (2018). Autonomous motility of polymer films. *Adv. Mater.* 30, 1705616. doi:10.1002/adma.201705616

Wu, J., Wu, Z., Wei, Y., Ding, H., Huang, W., Gui, X., et al. (2020). Ultrasensitive and stretchable temperature sensors based on thermally stable and self-healing organohydrogels. *ACS Appl. Mater Interfaces* 12, 19069–19079. doi:10.1021/acsami.0c04359

Yang, X. W., Qiu, L., Cheng, C., Wu, Y. Z., Ma, Z. F., and Li, D. (2011). Ordered gelation of chemically converted graphene for next-generation electroconductive hydrogel films. *Angew. Chemie-International Ed.* 50, 7325–7328. doi:10.1002/anie.201100723

Zhai, D. Y., Liu, B. R., Shi, Y., Pan, L. J., Wang, Y. Q., Li, W. B., et al. (2013). Highly sensitive glucose sensor based on Pt nanoparticle/polyaniline hydrogel heterostructures. *ACS Nano* 7, 3540–3546. doi:10.1021/nn400482d